STRUCTURAL ANALYSIS OF THE BRAZILIAN 14-X HYPERSONIC AEROSPACE VEHICLE AT MACH NUMBER 10

Felipe Jean da Costa, felipejean@ieav.cta.br
ITA - Instituto Tecnológico de Aeronáutica, Praça Marechal Eduardo Gomes, nº 50 Vila das Acácias CEP. 12.228-900 São José dos Campos, SP - Brasil

Israel da Silveira Rêgo, israel.rego@ieav.cta.br
Marco Antônio Sala Minucci, marco.salaminucci@gmail.com
Tiago Cavalcanti Rolim, tiagorolim@ieav.cta.br
Gianino Ponchio Camillo, giannino@ieav.cta.br
Antonio Carlos de Oliveira, acoc@ieav.cta.br
Paulo Gilberto de Paula Toro, toro@ieav.cta.br
IEAv - Instituto de Estudos Avançados, Trevo Coronel Aviador José Alberto Albano do Amarante, nº 1 Putim CEP. 12.228-001 São José dos Campos, SP - Brasil

Abstract. *The Brazilian VHA 14-X is a technological demonstrator of a hypersonic airbreathing propulsion system based on supersonic combustion (scramjet) to fly at Earth's atmosphere at 30 km altitude at Mach number 10, designed at the Prof. Henry T. Nagamatsu Laboratory of Aerothermodynamics and Hypersonics, at the Institute for Advanced Studies. Basically, scramjet is a fully integrated airbreathing aeronautical engine that uses the oblique/conical shockwaves generated during the supersonic/hypersonic flight, to promote compression and deceleration of freestream atmospheric air at the inlet of the scramjet. Scramjet is an aeronautical engine, without moving parts, therefore it is necessary another propulsion system to accelerate the scramjet to the operational conditions. Rocket engines are low-cost solution to launch scramjet integrated vehicle to flight at the test conditions. The Brazilian two-stage rocket engines (S31 and S30) are able to boost the VHA 14-X to the predetermined conditions for the scramjet operation, 30 km altitude but at Mach number 7. Therefore, it is needed to design the structure of the VHA 14-X waverider to support the aerodynamic loads during the atmospheric hypersonic flight at Mach number 10. Therefore, it is necessary design the structure of the 14-X waverider to support the aerodynamic loads during the atmospheric hypersonic flight at the conditions mentioned earlier. One-dimensional theoretical analysis, applied at 30 km altitude at Mach number 10, provide the pressure distribution over the 14-X waverider upper and lower surfaces. Structural materials for the stringers and ribs, and C-C as coating material were specified based on preliminary studies. Through the ANSYS Workbench software provides the Structural Numerical Analysis, using Finite Element Method, considering the 14-X waverider unpowered scramjet at 30 km altitude at Mach number 10, The results could be expressed in terms of the stress, strains and deformations.*

Keywords*: scramjet, waverider, Aerospace vehicle, Structural Analysis, 14-X waverider*

1. THE BRAZILIAN 14-X HYPERSONIC AEROSPACE VEHICLE

The Prof. Henry T. Nagamatsu Laboratory of Aerothermodynamics and Hypersonics, at the Institute for Advanced Studies, is developing the 14-X Hypersonic Aerospace Vehicle, 14-X waverider (Figure 1). The 14-X waverider is a technological demonstrator designed to demonstrate, during the hypersonic flight with speed corresponding to Mach number 10 through the Earth's atmosphere at 30 km altitude, two innovative technologies: waverider technology, to obtain lift from conical shockwave during the supersonic or hypersonic flight; and the scramjet engine that consists in a hypersonic airbreathing propulsion system based on supersonic combustion (Costa, 2014).

The scramjet engine during the hypersonic flight promotes the compression and deceleration of freestream atmospheric air, at the inlet of the scramjet, using the oblique/conical shockwaves. The scramjet is integrated to the vehicle to obtain the adequate air in supersonic speed conditions to burn fuel (in general, Hydrogen) in the combustion chamber. The scramjet engine is an aeronautical engine without moving parts, and due this fact it is necessary another propulsion system to accelerate the vehicle powered by scramjet up to operation conditions. Rocket engines represent the best solution, in technical and economic terms, to launch the powered vehicle by scramjet. The Brazilian two-stage rocket engines (S31 and S30) will accelerate the VHA 14-X to the predetermined conditions to start the scramjet at 30 km altitude, but at Mach number 7 (the maximum corresponding speed that S31 and S30 engines reaches).

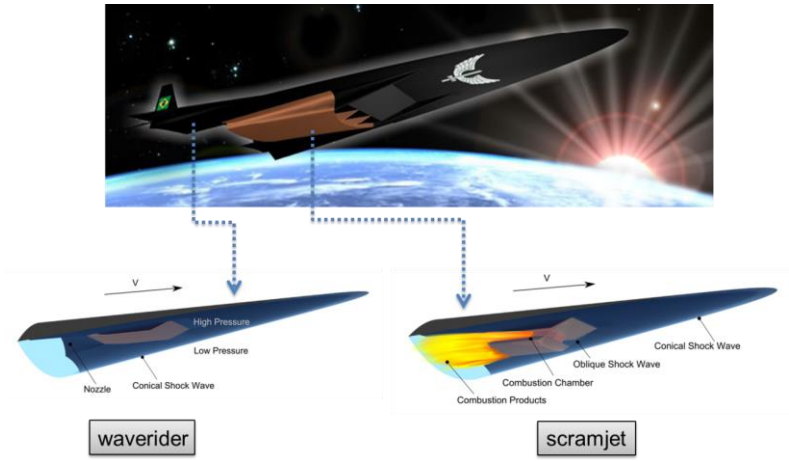

Figure 1. The 14-X Hypersonic Aerospace Vehicle with waverider and scramjet concepts (Costa, 2014).

2. STRUCTURAL ANALYSIS

In general, the structures of aerospace hypersonic vehicles consist of the combination of different structural elements (stringers, ribs, skins, etc.) and of different types of materials. Due to the high complexity of these aerospace structures, they cannot be described by approximated or by exact mathematical equations, invalidating the use of classical methods of structural analysis. Therefore, it is necessary the use of the numerical methods, such as, Finite Element Method (FEM) to describe the high complexity structures into simpler and easier algebraic equations (Lage, 2009). FEM has high degree of programmability, promoting higher solution speed and accuracy in calculations of the associated matrices.

2.1 Finite Element Method

The FEM resembles the finite difference method, but with more general presentation and it has greater power of solution in applications involving physical, geometrics and/or boundary conditions complexities. In the FEM the domain should be observed as an assembly of subdomains, where in each subdomain the government equations are approximated by any of the traditional variational methods. The approximated solution, provided by a set of subdomains, is the easy way to the representation of a complex function as a set of simple polynomial (Reddy, 2006).

The structural domain can be classified into three categories, one-dimensional (line elements), two-dimensional (triangular and quadrilateral elements) and three-dimensional (tetrahedral, prismatic, and hexahedral elements, or a combination of any three-dimensional elements) (Gupta and Meek, 2003). Figure 2a shows the domain Ω, which is geometrically more complex than the Figure 2b, which is represented by a set of geometrically simpler subdomains, called finite elements. In general, one may divide the domain Ω (Figure 2a) in some subdomains Ω_c (Figure 2b) in order to obtain the solution. The FEM uses mathematical modeling and the governing equations inherent to the problem may be applied to the each individual elements Ω_c of the Figure 2b, and by the superposition of the each individual finite element of Figure 2c, one can obtain the global behavior of the structure presented by Figure 2d, that represents the final result of this domain.

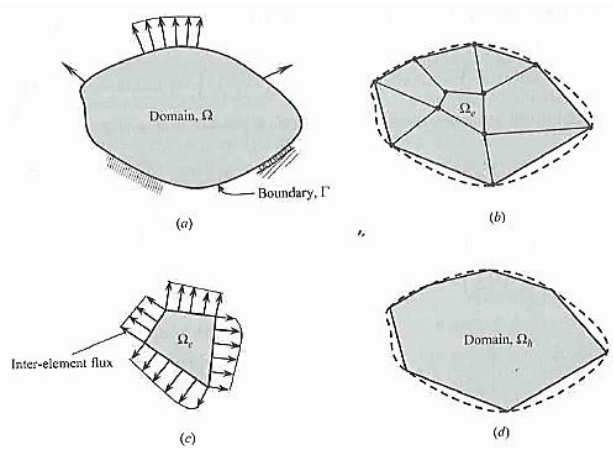

Figure 2. Two-dimensional representation of the domain by a set of triangles and quadrilaterals (Gupta and Meek, 2003).

2.1 Finite Element Method in Mechanics

From the theory of elasticity we may obtain the matrix equations for the numerical methods. The linear analysis uses the small strain theory, which considers small displacements and rotations, and the linear elastic behavior of the material submitted to the loads, stress and strain (Gupta and Meek, 2003). The three-dimensional formulation of Hooke's law expresses the total strain for the linear anisotropic material as follow:

$$\in = \in_E + \in_T + \in_I = C\sigma + \in_T + \in_I \tag{1}$$

where $\in_E$ is the elastic strain, σ is the stress vector, C is the constitutive relationship, $\in_T$ is the thermal strain vector, and $\in_I$ is the initial strain vector.

One may obtain the stress vector σ as function of the strain, given by:

$$\sigma = D \in -D \in_T -D \in_I \tag{2}$$

where, D is the stress-strain matrix, and may be obtained by $D = \frac{1}{c}$.

The matrix D is symmetric and for anisotropic materials it has 21 independent constants, as follow:

$$D = \begin{bmatrix} d_{11} & d_{12} & \dots & d_{16} \\ & d_{22} & \dots & d_{26} \\ \vdots & \vdots & \ddots & \vdots \\ & sym & \dots & d_{66} \end{bmatrix} \tag{3}$$

Considering orthotropic materials with three orthogonal planes of symmetry, the stress-strain matrix D has a reduction for nine independent constants (six elements in the D_{11} and three in the D_{22}), produced by the relationship, as presented in the equation 3.

$$D = \begin{bmatrix} D_{11} & 0 \\ 0 & D_{22} \end{bmatrix} \tag{4}$$

For anisotropic materials in problems involving shell and plate we can write stress-strain relationship as:

$$\begin{bmatrix} \sigma_{xx} \\ \sigma_{yy} \\ \sigma_{xy} \\ \sigma_{yz} \\ \sigma_{zy} \end{bmatrix} = \begin{bmatrix} d_{11} & d_{12} & d_{14} & 0 & 0 \\ & d_{22} & d_{24} & 0 & 0 \\ & & d_{44} & 0 & 0 \\ & & sym & d_{55} & d_{56} \\ & & & & d_{66} \end{bmatrix} \begin{bmatrix} \in_{xx} \\ \in_{yy} \\ \in_{xy} \\ \in_{yz} \\ \in_{zy} \end{bmatrix} \tag{5}$$

For orthotropic materials and considering plane stress problems the Eq. 5 suffer a reduction to its first 3x3 submatrix as shown below:

$$\begin{bmatrix} \sigma_{xx} \\ \sigma_{yy} \\ \sigma_{xy} \end{bmatrix} = \begin{bmatrix} \frac{E'_{xx}}{\left(1 - n' v'^2_{yx}\right)} & \frac{v'_{yx} E'_{xx}}{\left(1 - n'' v'^2_{yx}\right)} & 0 \\ sym & \frac{E'_{yy}}{\left(1 - n' v'^2_{yx}\right)} & 0 \\ & & G_{xy} \end{bmatrix} \begin{bmatrix} \in_{xx} \\ \in_{yy} \\ \in_{xy} \end{bmatrix} \tag{6}$$

where, ν'^{2}_{yx} is the Poisson's ratio and $n' = E'_{xx} / E'_{yy}$.

For layered anisotropic materials the relationship is formulated by stress transformation matrix T_σ and expressed in vector form as:

$$\sigma' = T_\sigma \sigma \tag{7}$$

3. STRUCTURAL ANALYSIS PROCEDURE

The current analysis was performed as a static structural type, and the methodology for the pre-processing and post-processing were defined to maximize the efficiency in the achievement of the results at the structural analysis of the 14-X waverider coupled to the rocket engines (S31 and S30) flying at 30 km altitude at speed corresponding to the Mach number 10. The pre-processing consists of the following steps: add materials properties to the ANSYS material database; application of the APDL (ANSYS Parametric Design Language) commands for the Carbon-Carbon parts; import the CAD geometry of the 14-X waverider to ANSYS Workbench platform; mesh generation by ANSYS meshing; optimization of the mesh by the quality analyzing; dimensional parameterization; adding supports to the Finite Element Model (Structure); determination and application of the loads (provided aerodynamic analysis). The post-processing consists in the stress and total displacement analysis in order to optimize the thickness and weight reduction in the areas of low stress in the structural components of the 14-X waverider. If necessary, should be considered changes in the geometry and the pre-processing and post-processing process need to be repeated up to obtain an appropriated solution.

3.1 Mesh

The automatic mesh given by ANSYS Workbench (Meshing) over the 14-X waverider presented some degenerated elements, which it is characteristic of the non-structured mesh, and can generate non-adequate results, by the presence of some numerical singularities.

Appropriate tools provided by ANSYS Workbench software were used to treat the mesh, such as element sizing, number of division, method, error evaluating, etc. The optimized mesh (Figure 3) containing 184632 nodes and 61619 elements (hexahedral and tetrahedral) were obtained using the 14-X waverider geometry implemented in the ANSYS software.

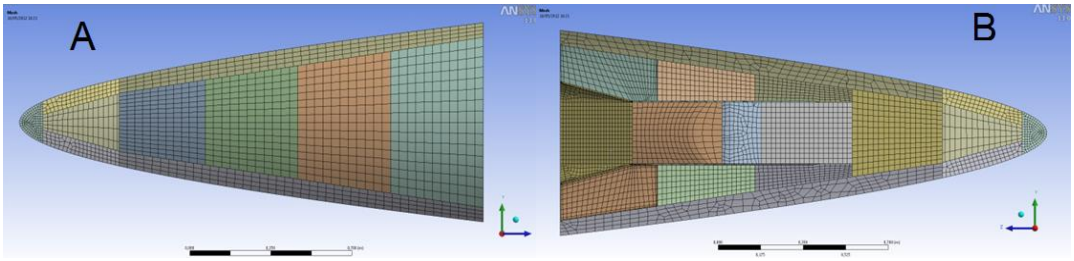

Figure 3. VHA 14-X treated mesh over upper (A) and lower (B) surfaces (Costa, 2013).

In the numerical analysis, the mesh element type is very important due the formulation and the physical application type. In the present case were used the SOLID186 and SOLID187 from the ANSYS Workbench.

The SOLID186 presents a quadratic displacement behavior and it is a higher order 3-D 20-node solid element. The element is defined by 20 nodes with three degrees of freedom per node and the nodal translations in the x, y, and z directions. The element allows plasticity, stress stiffening, creep, hyperelasticity, large deflection, and large strain capabilities. The formulation includes mixed capability for simulating deformations of nearly incompressible elastoplastic materials, and fully incompressible hyperelastic materials. An alternative to low order precision version is to use the SOLID185.

SOLID187 element is a higher order 3-D, 10-node element. SOLID187 has a quadratic displacement behavior and is well suited to modelling irregular meshes (such as those produced from various CAD/CAM systems). The element geometry is defined by 10 nodes, three degrees of freedom per node and translations in x, y, and z directions. The element capabilities comprise plasticity, hyperelasticity, creep, stress stiffening, large deflection, and large strain. For simulating deformations of nearly incompressible elastoplastic materials, and fully incompressible hyperelastic materials. The SOLID187 element uses the mixed formulation.

The ANSYS Workbench software in order to provide a more accurate answer, offers an error result based on stresses. The error resource helps us to identify the regions of high error and thus show where the model needs a more refined mesh. Moreover, the error result is restricted only for isotropic materials. Based on the error result a mesh

convergence was conducted, and some assumptions were assumed, such as the replacement of C-C parts for isotropic materials, in this case the material used was the Inconel 718.

3.2 Contacts

Computational structural analysis using FEM for a complete system (assembly), in which there is an interaction between the parts of the finite element model (mesh), is necessary the introduction of the information of the existence, or of possible existence, of the contact between parts. The pair added contacts must represent the physics of the problem, such as welded joints, bonded, bolted, riveted, etc.

In the present work it was selected the called "Bonded" contact, representing the surfaces to be stuck together, not allowing relative movement between them, i.e., does not allow the separation, penetration of surfaces or tangential movements, defining the regions "Contact" and "Target", as shown in Figure 6.

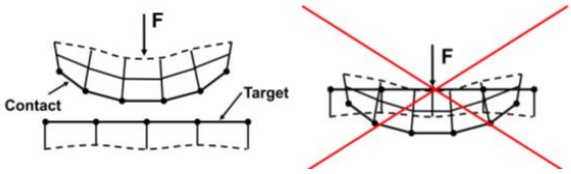

Figure 6. Penetration not allowed in the contact (Ansys, 2012).

Consequently, to prevent penetration between bodies, the mathematical formulation is one of the parameters that deal with the kinematics of the contact. For this study it was considered the "Pure Penalty" formulation, being based on the method of penalties, which is applied to the normal direction of the contact, assuming that the normal force is given by the contact stiffness (given the normal direction) multiplied by displacement, i.e., penetration, as shown in the following equation.

$$F_n = k_n x_p \tag{8}$$

The method of penalties allows a certain degree of penetration, knowing that the normal force is zero when there is lack of penetration. The contact stiffness will determine the amount of penetration, and the higher stiffness, to the lower penetration (Figure 7).

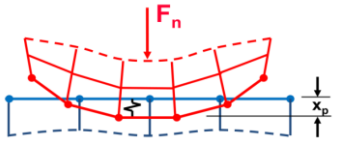

Figure 7. Contact Stiffness (Ansys, 2012).

3.3 Boundary-conditions

Based on previous works (Costa 2011; 2013), the structural materials selected for the VHA 14-X (Figure 8), are the special steel 4140 for the stringers, the stainless steel 304 for the ribs, the tungsten to the conical nose, the Carbon-Carbon (C-C) for the leading edges and for the passive thermal protection system (all skins) and Inconel 718 for the scramjet engine.

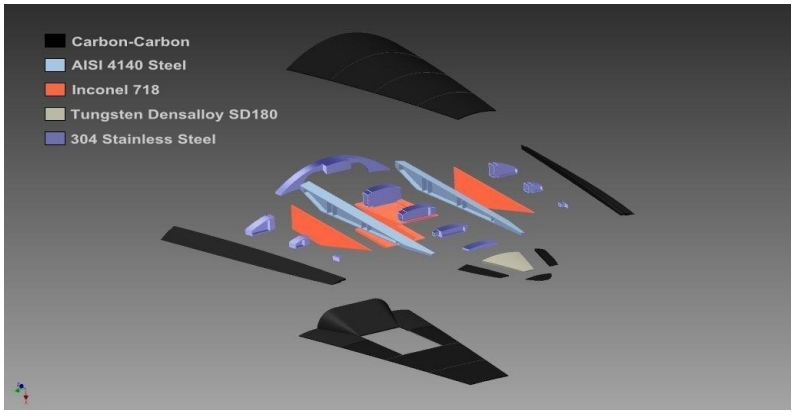

Figure 8. VHA 14-X material specification and layout, adapted from Costa, 2011.

The Table 1 presents the isotropic and non-isotropic material mechanical properties, respectively, specified by Costa (2011) to be used at the structural and thermal protection systems of the VHA 14-X (Figure 8). These mechanical properties were inserted into ANSYS Workbench material database. The mechanical properties of the C-C 3D orthogonal (Table 2) were obtained from (Gonçalves, 2008).

Table 1. Structural Mechanical properties for isotropic material (Costa, 2011).

MATERIAL	ρ [g/cm³]	E [GPa]	υ	σ_e [MPa]	σ_r [MPa]
Steel 4140	7.85	20.5	0.29	415	655
Stainless Steel 304	8	20	0.29	215	505
Inconel 718	8.19	20.49	0.284	980	1100
Tungsten	17.75	40	0.28	552	827

Table 2. Structural Mechanical properties of the Carbon-Carbon orthogonal, updated (Costa, 2011).

PROPERTY	C-C 3D orthogonal
Ex [GPa]	31.8
Ey [GPa]	31.8
Ez [GPa]	38.5
Gxy[GPa]	7.8
Gxz[GPa]	5.0
Gyz[GPa]	5.0
υxy	0.1306
υxz	0.0670
υyz	0.0670

The boundary conditions (Figure 9) applied to the static structural analysis are the aerodynamic load evaluated for the lower and upper surfaces of the VHA 14-X flying (with no angle of attack) at 30 km altitude with speed correspondent to Mach number 10, and the inherent bonds (VHA 14-X coupled to the 2nd stage of the S31 and S30 rocket engines) of the structure to each region (and components). Additionally, it was inserted the acceleration of 14g's (Figure 9), being 13g's correspondent to the acceleration reached during the atmosphere flight of the rocket engines and 1g's to the Earth's gravitational acceleration.

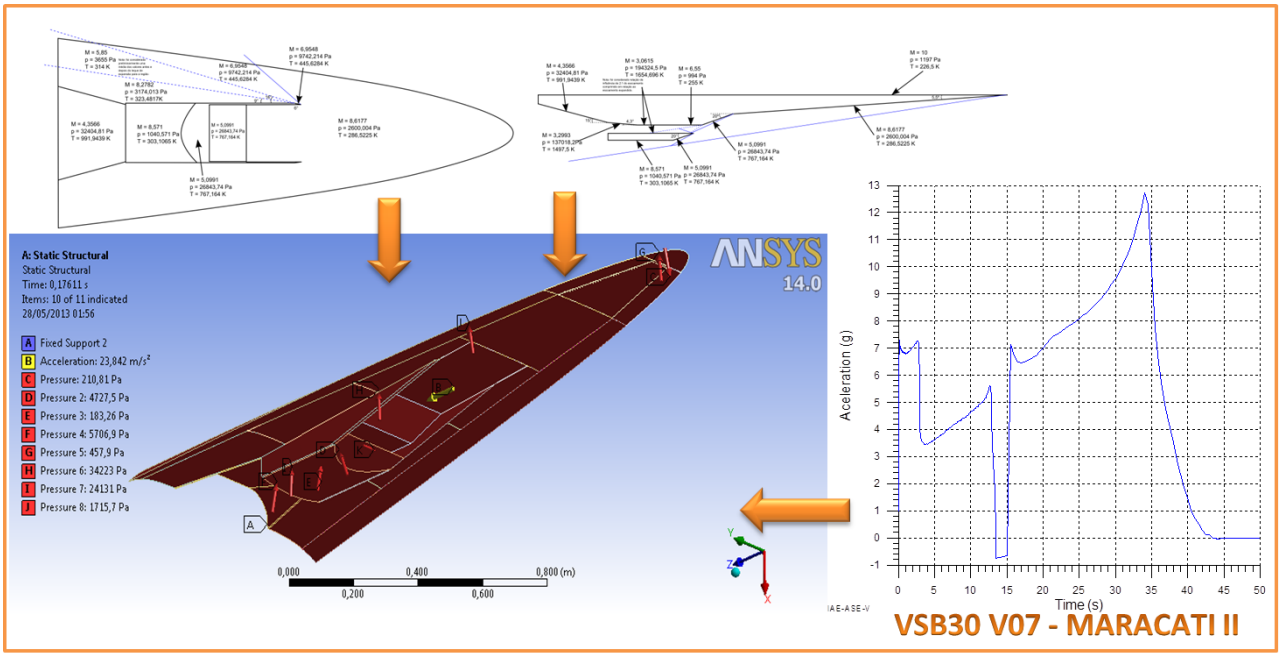

Figure 9. Boundary-conditions (acceleration, support and pressures) applied to the VHA 14-X.

4. RESULTS

Structural Numerical Analysis using Finite Element Method has been applied to the VHA 14-X waverider unpowered scramjet flying at 30 km altitude at Mach number 10, considering the dynamic pressure during the ballistic

trajectory of the S31 and S30 unguided, rail launched, solid rocket engines. Considering the boundary conditions of the aerodynamic load (Fig. 9), acceleration of 14 g's and the mechanical isotropic materials (Table 1) and mechanical orthotropic materials (Table 2).

The maximum and minimum equivalent stresses (von Mises) are 135 MPa and 6.73 10^{-3}, respectively (Fig. 10A). The maximum equivalent stress occurs at the stringers close to the end (trailing edge) of the vehicle (red color) and minimum occurs close to the leading-edge of the vehicle (blue color) at the upper surface (Fig. 10A). However, maximum and minimum equivalent stresses found in the present evaluation are lower than any selected materials yield stress (Tables 1 and 2).

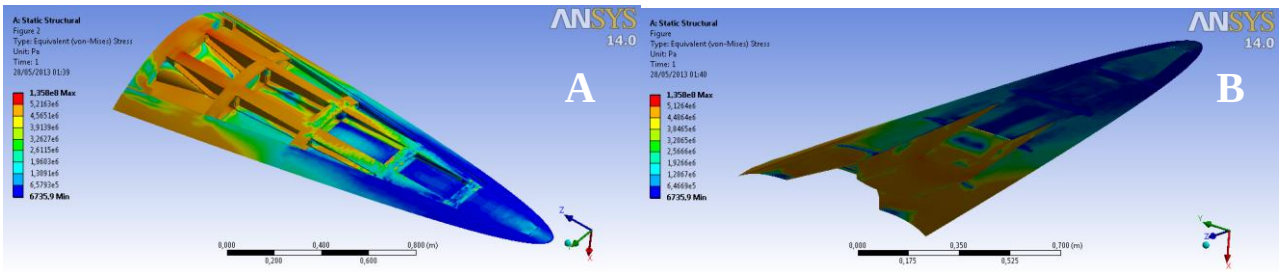

Figure 10. Equivalent stress (von Mises) fields at the internal structure (A) and lower surface (B) of the VHA 14-X waverider at Mach 10.

The x-direction deformation reached the maximum of 2.565 10-7 m and minimum of -3.65 10-3 m (Fig. 11A). The maximum and minimum y-direction deformations are 7.75 10-5 m and -9.95 10-5 m (Fig. 11B), respectively. Finally, maximum and minimum z-direction deformations are (Fig. 11C) 1.16 10-4 m and -2.18 10-4 m for Mach number 10, respectively.

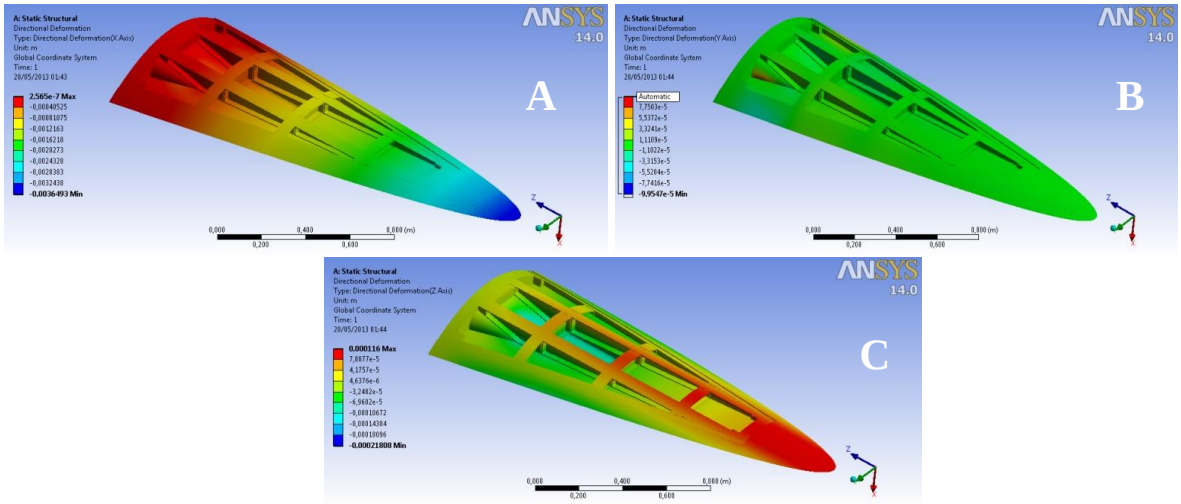

Figure 11. *x*-direction (A), *y*-direction (B) and *z*-direction (C) deformations of the structure of the VHA 14-X at Mach 10.

The "Fixed Support" bond used in the present structural analysis, does not allow the deformation between two adjacent components related to the initial position. Therefore, the deformation is related to the global coordinates.

Figure 12A shows the total deformation of 3.65 10^{-3} m which occurs at the leading-edge of the VHA 14-X, considering the boundary conditions of the aerodynamic load (Fig. 9), acceleration of 14g's (Fig. 9) and the mechanical isotropic materials (Table 1) and mechanical orthotropic materials (Table 2).

The principal elastic strain shows the equivalent deformation which occurs in the elastic region of the material used at the each components of the VHA 14-X waverider. The maximum principal elastic strain of 1.03 10-4 m/m and minimum of -3.54 10-6 m/m is showed in the Fig. 12B, for Mach number 10.

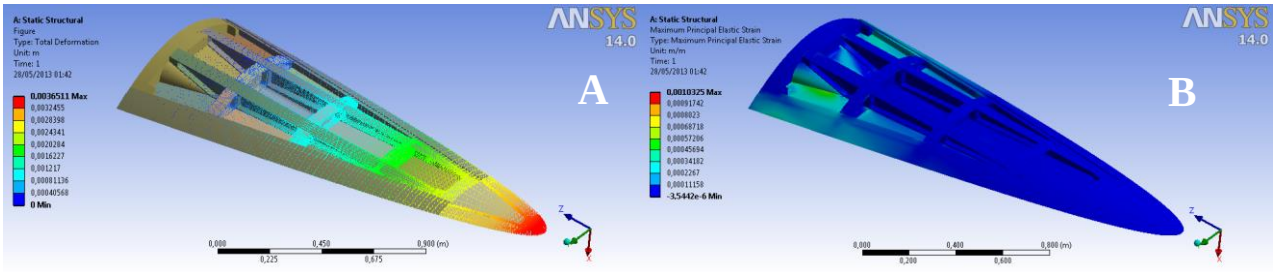

Figure 12. Total deformation (A) and Principal elastic strain (B) of the structure of the VHA 14-X at Mach 10.

5. CONCLUSIONS

The VHA 14-X structure analysis presents an excellent response to the structural loads faced during the atmospheric flight at 30 km altitude at Mach number 10. Regarding to the stress field, note that the maximum is and 135 MPa, which is focused on the rear of the vehicle (trailing edge), that is in according with the adopted methodology for boundary conditions. Note that the maximum stress in the structure is lower than yield limits of selected materials, and thus, no plasticity effects will occur. The directional deformation results are concerned with the applied loads, principally in the z axis, in which the rear of the vehicle experiments the maximum deformation. All directional deformation such as the total deformation (being a combination of directional deformations) is within an acceptable range. The principal elastic strain is within satisfactory limits, not burdening any structural component.

6. ACKNOWLEDGEMENTS

The last author would like to express gratitude to FINEP (project nº 0445/07), to CNPq (project nº 471345/2007-5) and to AEB (project nº 25/2009-1) for the financial support for the 14-X Hypersonic Aerospace Vehicle design and experimental investigations. The first author would like to thank the CNPq (process nº 376505/2014-1), for the financial support.

7. REFERENCES

Ansys. Help. 2012

Costa, F. J., 2011, Projeto Dimensional para Manufatura do Veículo Hipersônico Aeroespacial 14-X (in Portuguese). Undergraduate Work, FATEC de São José dos Campos: Professor Jessen Vidal, Brazil.

Costa, F. J. ; Toro, P. G. P. ; Rolim, T. C. ; Camillo, G. P. Brazilian 14-X Hypersonic Waverider Upowered Scramjet Aerospace Vehicle Structural Analysis At Mach Number 7. In: COBEM- 22nd International Congress of Mechanical Engineering, 2013, Ribeirão Preto. 22nd International Congress of Mechanical Engineering, 2013.

Costa, F. J., 2014. Thermo-Structural Analysis of the Brazilian 14-X Hypersonic Aerospace Vehicle. Master thesis, Instituto Tecnológico de Aeronáutica, São José dos Campos, Brazil.

Gonçalves, A. Caracterização de Materiais Termoestruturais a Base de Compósitos Carbono Reforçados com Fibras de Carbono (CRFC) e Carbonosos Modificados com Carbeto de Silício (SiC). 2008. 226 p. Tese de doutorado – Instituto Tecnológico de Aeronáutica, São José dos Campos.

Gupta, K. K. e Meek, J. L. Finite element multidisciplinary analysis. 2ª ed. AIAA Education Series, 2003.

Lage, Y. E. Análise Estrutural à Asa da aeronave Lockheed Martin C-130H. 90 f. Tese (Mestrado em Engenharia Aeroespacial) – Universidade Técnica de Lisboa, Lisboa, 2009.

Reddy, J. N. and Gartling, D. K. The Finite Element Method in Heat Transfer and Fluid Dynamics, Ed. 3, CRC Press, Taylor & Francis Group, Boca Raton, 2010

8. RESPONSIBILITY NOTICE

The authors are the only responsible for the printed material included in this paper.